Kinetics and Reactive Mixing: Fragmentation and Coalescence in Turbulent Fluids

Giridhar Madras
Dept. of Chemical Engineering, Indian Institute of Science, Bangalore 560 012, India

Benjamin J. McCoy
Dept. of Chemical Engineering, Louisiana State University, Baton Rouge, LA 70803

DOI 10.1002/aic.10098
Published online in Wiley InterScience (www.interscience.wiley.com).

Reactive mixing in liquids can be quantitatively described by combining chemical kinetics and hydrodynamics so that dispersed reactants interact at evolving fluid–element interfaces. For the batch reactor we postulate that the dispersed fluid elements are fragmented in a cascade of increasingly smaller sizes and larger interfacial area. The reversible fragmentation–coalescence is described by a population dynamics equation that has an exact self-similar solution for the size distribution as a function of time. Two types of competitive reaction kinetics incorporating a diffusion-limited fast reaction satisfy nonlinear differential equations, written in terms of moments of the time-dependent dispersed-fluid size distribution. Applying a compressed time variable to transform to a simple system of differential equations readily solves the nonlinear equations. The straightforward solutions display realistic effects of dispersed fluid volume fraction, rate parameters, and initial concentrations. Final fractional conversions, occurring when the limiting reactant is depleted, are functions of a Damkohler number, volume fraction of dispersed reactant, and scaled initial conditions. © 2004 American Institute of Chemical Engineers *AIChE J,* 50: 835–847, 2004
Keywords: reactive mixing, Damkohler number, batch reactor, fragmentation, coalescence

Introduction

Mixing in reactors is a challenging problem in chemical kinetics and reaction engineering that has attracted numerous attempts at quantitative description through either empirical methods or fundamental theory. The interaction of chemical reactions and vessel fluid mechanics, usually involving turbulence, combine to cause significant complexity. Mixing occurs by intermingling of fluid elements that are being sheared and merged on space and time scales from molecular to macroscopic. Experiments in reactive mixing are typically conducted by allowing reactants, say A and B, to enter the reactor separately and then measuring their conversion for different mixing conditions. The reaction occurs by contact of A and B at the interface between fluid elements, or by diffusion of a reactant into an adjacent fluid element. In reaction experiments one of the reactants will be dispersed into the other, thus allowing identification with two-phase reactors in which one phase fragments and/or coalesces. The mathematics of population dynamics can then be applied to describe how fluid elements are dispersed so that reaction occurs at their evolving interfaces.

Chemical engineers have devised several approaches to model reactive mixing (Baldyga and Bourne, 1999; Ottino et al., 1999; Sundaresan, 2000). In the most common textbook approach (Levenspiel, 1999), pairs or networks of continuous-flow stirred tank (CSTR) and plug-flow reactors (PFR) are

Correspondence concerning this article should be addressed to G. Madras at giridhar@chemeng.iisc.ernet.in.

assembled empirically to combine regions of perfect mixing (CSTR) with regions lacking mixing (PFR). Connected compartments can also be inserted to blend in dead regions with mass transfer or flow. Elaborate assemblages of reactor elements have been proposed to describe heterogeneous mixing (Başağaoğlu et al., 2002). The two-mode model (Chakraborty and Balakotaiah, 2002) is a more sophisticated approach that involves coupled balance equations for the mixing-cup and spatially averaged concentrations, and the exchange between these two modes. The slab diffusion model (Li and Toor, 1986) postulates that mixing is governed by molecular diffusion between layered slabs of constant thickness δ_s. The thickness parameter δ_s depends on fluid dynamics for the basic model. For the modified versions (Baldyga and Bourne, 1999), δ_s is influenced additionally by the diffusivity, or its thickness varies with time. The closure model has its roots in the classical idea that turbulence consists of fluctuations in fluid properties (Baldyga and Bourne, 1999; Fox, 1992). A first-order perturbation scheme provides a way to time-smooth the transport equations, resulting in expressions that require a closure scheme, usually involving constitutive rate expressions (Baldyga and Bourne, 1999; Dutta and Tarbell, 1989).

At the heart of this complex problem are turbulence concepts, which can provide a guiding framework for constructing realistic models. The following arguments assist in defining the model that we propose. The characteristic features of turbulence (Frisch and Orszog, 1990) are randomness, eddy viscosity, hierarchical cascading, and scaling. Fragmentation as described by population balance equations is consistent with these characteristics.

(1) Fragmentation is random when the random breakage kernel is used in the population dynamics equation to describe the evolving fluid elements. The distributed products for binary fragmentation are random in size, and furthermore the population balance equations are independent of spatial position so that fluid elements are randomly distributed in the vessel.

(2) The eddy viscosity is based on an analogy with the molecular explanation for kinematic viscosity, thus ascertaining the diffusive properties of turbulent dynamics. If the eddy viscosity is postulated to be of the order of the root-mean-square value of the fluctuating velocity times a length scale (or mixing length), then the ratio of eddy viscosity to kinematic viscosity is a Reynolds number. The fundamental mixing length concept is basic to the heterogeneous nature of turbulence, here manifested by fluid elements formed through fragmentation. In a typical stirred vessel, regions near the impeller will undergo intense shearing, whereas other regions will be less agitated. It is thus reasonable to use reversible fragmentation, so that breakup and agglomeration occur concurrently to account for different regions where turbulent shearing and coalescence vary in strength. As a refinement and extension of the present treatment, such regions could be modeled as connected compartments.

(3) The notion that turbulence is based on fragmentation leads naturally to a hierarchical structure based on fluid elements (eddies) that are generated from larger eddies and in turn generate smaller eddies. Consistent with the reversible nature of fragmentation, the cascade can be reversed in regions where lower power input and lower shear rates allow coalescence and therefore larger fluid elements. Laminar mixing, by contrast, lacks eddy fluctuations and thus stretches, but does not fragment, the fluid elements.

(4) Population dynamics yields the fluid-element (eddy) size distribution, and hence an average eddy mass, which is simply related to the mixing length through the fluid density. Kolmogorov's scaling theory shows how the mixing length is related to the vessel Reynolds number. This suggests a relationship for the fragmentation rate parameters in terms of the vessel Reynolds number, thus providing a connection between fragmentation kinetics and reactor vessel parameters. In reactive mixing the Damkohler number is related to vessel geometry through the energy dissipation rate (Baldyga and Bourne, 1999).

The model we propose has similarities to the coalescence and redispersion model of Rietema (1958) and Curl (1963) as explained by Baldyga and Bourne (1999). This model was based on many fluid elements of equal volumes that could coalesce pairwise, instantaneously mix reactants within the new elements mainly by diffusion, and immediately fragment into equal sized daughter elements. Our current model invokes a more detailed and complex coalescence–fragmentation mechanism that provides for an increase in number of dispersed fluid elements, and thus an enhanced contact with the continuous fluid. The increased contact among fluid elements is the essence of reactive mixing, and appears also in laminar processes (for example, Szalai et al., 2003). Other variations have led to engulfment and IEM (interaction by exchange with the mean) models, described by Baldyga and Bourne (1999; pp. 561 and 552, respectively).

Our objective is to study reaction kinetics during mixing of miscible liquids by extending and generalizing our recent work (McCoy and Madras, 2003a) on chemical kinetics in two-phase reactors with simultaneous fragmentation and coalescence. We hypothesize that the basic concept can be applied to miscible liquids or to liquid–liquid, gas–liquid, or solid–liquid systems. Our previous model (McCoy and Madras, 2003a) considered two immiscible phases, one identified as the dispersed phase subject to simultaneous coalescence and breakup. The model extends fundamentally the macromixing concept (Levenspiel, 1999) based on a stable dispersed phase that neither fragments nor aggregates. In the prior work, we considered various reactions, all occurring at the interface between dispersed and continuous phases. The reaction conversion depended on whether fragmentation or coalescence dominated. Reaction rate computations were considerably simplified when the dispersed phase obeyed the exact similarity solution to the population dynamics equation. The work demonstrated how chemical reaction mass balances could be combined with distribution kinetics (and population dynamics) to extend chemical reaction analysis.

All approaches to laminar and turbulent mixing have the problem of describing how a fluid is dispersed into another fluid. When the fluids are miscible, the usual experimental method is to dye the dispersed fluid and observe its breakup and dispersal into the undyed fluid. Because miscible fluids lack surface tension at the interfaces, the rates of breakup and coalescence will certainly be different from those of immiscible fluids. But we argue that the dispersal can be represented by population dynamics, with reasonable assumptions about the shape of the fluid elements. Clearly, interdiffusion must be a key issue for such mixing, and this is the reason that the Damkohler number is central to reactive mixing models.

The present project is concerned with mathematically describing fluid-mixing experiments reported in the literature. Important to chemical manufacture and to research in reactive mixing, parallel (consecutive) reactions are characterized by a product distribution that is strongly influenced by mixing (Bourne and Yu, 1994; Li and Toor, 1986). With simple macromixing, reaction occurs at the constant-area interface and faster reactions dominate the kinetics. When micromixing increases, however, the interface becomes more extensive allowing slower reactions to have an influence. As fragmentation proceeds in the absence of significant coalescence, the micromixing limit would be reached, in which reactants are dispersed at the molecular level. Thus the time-dependent reaction model based on fragmentation kinetics is a plausible quantification of reactive mixing dynamics, and our aim is to explore its predictions.

In the present work we focus on competitive reactions among reactants whose molecules must come into proximity for the bimolecular reaction to occur (Baldyga and Bourne, 1999; Bourne and Yu, 1994; Chakraborty and Balakotaiah, 2002; Levenspiel, 1999; Li and Toor, 1986). Both fragmentation and coalescence are incorporated into the theory, and chemical reaction is considered to occur at the interfaces of the dispersed fluid elements. Perfect mixing is attained when fragmentation of the dispersed phase reduces the size of fluid elements to molecular scale such that immediate reaction is facilitated. Realistically, this molecular-scale mixing cannot occur instantaneously, but will proceed over a time that is expected to decrease with increasing fragmentation rate. The efficacy of mixing depends on geometric, hydrodynamic, and fluid properties, as embodied for example in the Reynolds number. Perfect segregation is the case when fluid elements are unchanging and reaction occurs at the static interface. The present theory accounts for the temporal evolution of the reaction by representing the contact among fluid elements that intermingle by the mixing process. The extension of the theory to flow reactors is straightforward, and for the steady-state plug-flow reactor is simply a replacement of time with longitudinal distance divided by velocity.

An objective of this investigation is to model the kinetics of a stirred batch reactor for two specific competitive reactions, which have been reported for stirred vessels by Bourne and Yu (1994) and for tubular reactors by Li and Toor (1986), who performed experiments with jets of one reactant dispersed into the second reactant flowing parallel to the jet streams. In all mixing the dispersed elements undergo shearing and some coalescence as the fluids are convected within the vessel or along the reactor tube length. Following other studies (Curl, 1963; Rietema, 1958) we consider that reactant concentration is uniform within all dispersed fluid elements; thus diffusion inside the fluid elements is assumed rapid relative to breakage–coalescence rates. A distribution kinetics approach (McCoy and Madras, 1998, 2002, 2003b) describes the time evolution of the dispersed-element mass distribution. Given an initial distribution, the reversible breakage–aggregation kinetics causes the distribution to evolve to a final steady state, where binary fragmentation and coalescence are balanced in a dynamic equilibrium. The evolution of the size distribution and the final dynamic equilibrium will depend on the rate coefficients chosen for fragmentation and coalescence. An analytical similarity solution (McCoy and Madras, 1998, 2002, 2003b) is possible when the fragmentation rate is directly proportional to the element mass and the coalescence rate is independent of element mass. For other forms of the rate-coefficient dependency on element mass, however, an analytical solution is not possible and numerical methods have to be applied. For simultaneous fragmentation and coalescence, we show the time evolution of the reactant and product concentrations, and hence of the selectivity, when the overall rate is controlled by the interfacial area. In addition to the fragmentation–coalescence parameters, which reflect hydrodynamics, the reaction yields depend on the kinetic rate parameters and initial reactant concentrations. Computations for concentration time dependency and for final yields of the competing reactions, determined when the limiting reactant A is exhausted, are relatively straightforward.

Distribution Kinetics

Consider that fluid elements $P(x)$ undergo shearing and merging in the turbulent stirred tank. When fragmentation and coalescence are uncorrelated, the simultaneous binary processes can be represented as

$$\mathbf{P}(x) \underset{k_a(x', x-x')}{\overset{k_b(x)}{\rightleftharpoons}} \mathbf{P}(x') + \mathbf{P}(x - x') \tag{1}$$

where $k_b(x)$ and $k_a(x', x - x')$ represent the rate coefficients for fragmentation (breakage) and coalescence (aggregation), respectively. The distribution is defined so that $p(x, t)dx$ is the number of dispersed fluid elements per vessel volume at time t in the mass range $(x, x + dx)$. It follows that $xp(x, t)dx$ is the mass of such elements per volume. The moments consequently are defined by

$$p^{(\nu)}(t) = \int_0^\infty p(x, t)x^\nu dx \tag{2}$$

The number of fluid elements per vessel volume is $p^{(0)}(t)$. The dispersed-fluid volume fraction, α, is related to $p^{(1)}(t) = p_0^{(1)}$, the constant mass per vessel volume, and its mass density, ρ, as $\alpha = p_0^{(1)}/\rho$. The population balance equation (PBE) is first-order for breakage and second-order for aggregation (McCoy and Madras, 1998),

$$\partial p(x, t)/\partial t = -k_b(x)p(x, t) + 2\int_x^\infty k_b(x')p(x', t)\Omega(x, x')dx' - 2p(x, t)\int_0^\infty k_a(x, x')p(x', t)dx' + \int_0^x k_a(x', x - x')p(x', t)p(x - x', t)dx' \tag{3}$$

The initial distribution is $p(x, t = 0) = p_0(x)$, which by Eq. 2 has moments, $p_0^{(\nu)}$. The population dynamics Eq. 3 reduces to pure fragmentation or pure aggregation, respectively, when k_a or k_b is zero. The stoichiometric kernel, $\Omega(x, x')$, gives the

product mass distribution for the binary fission and satisfies symmetry and normalization conditions. A general fragmentation stoichiometric kernel has been proposed (McCoy and Wang, 1994) that can represent the range of product distributions from random to midpoint fission, $1/x'$ (chosen for the present study) and $\delta(x - x'/2)$, respectively. In general, the breakage rate coefficient $k_b(x)$ will increase with the size of the fragmenting element, for example, as x^λ (here, $\lambda = 1$ is assumed). We consider the aggregation rate coefficient independent of the masses of the coalescing elements, thus, in the present work we let $k_a(x', x - x') = k_a$, a constant. More general rate coefficients can be handled by solving Eq. 3 numerically (McCoy and Madras, 2002). Because reactive mixing is dominated by fragmentation, this approximate treatment of coalescence should be reasonable.

It is advantageous to convert to dimensionless variables and parameters. The fragmentation rate coefficient, $k_b(x)$, requires that its mass dependency be represented explicitly. Following earlier work we define a reference breakage rate coefficient for elements of mass $p_0^{avg} = p_0^{(1)}/p_0^{(0)}$, such that $k_{bo} = k_b(x = p_0^{avg})$ and write the dimensionless quantities as follows (McCoy and Madras, 2002). The distributions are scaled with the initial quantities $p_0^{(0)}$ and p_0^{avg}

$$\kappa_b(\xi) = k_b(x)/k_{bo}, \quad \gamma = k_a p_0^{(0)}/k_{bo}, \quad \theta = tk_{bo},$$
$$\xi = x/p_0^{avg}, \quad P(\xi, \theta)d\xi = p(x, t)dx/p_0^{(0)}$$
$$P(\xi, \theta) = p(x, t)p_0^{avg}/p_0^{(0)}, \quad P^{(\nu)}(\theta) = p^{(\nu)}(t)/p_0^{(0)}(p_0^{avg})^\nu \tag{4}$$

The parameter γ is a measure of coalescence rate relative to the breakage rate. The population dynamics Eq. 3 reduces to

$$\partial P(\xi, \theta)/\partial\theta = -\kappa_b(\xi)P(\xi, \theta) + 2\int_\xi^\infty \kappa_b(\xi')P(\xi', \theta)\xi'^{-1}d\xi'$$
$$- 2P(\xi, \theta)\gamma\int_0^\infty P(\xi', \theta)d\xi' + \gamma\int_0^\xi P(\xi', \theta)P(\xi - \xi', \theta)d\xi' \tag{5}$$

For a scaled distribution $P(\xi, \theta)$, the reaction rate is determined by the νth moment, defined as

$$P^{(\nu)}(\theta) = \int_0^\infty \xi^\nu P(\xi, \theta)d\xi \tag{6}$$

When $\nu = 2/3$ the moment represents a measure of the total interfacial area. Thus $P^{(2/3)}$ will increase with time if breakage is predominant, and will decrease if agglomeration dominates. We assume a power relationship for the breakage rate, $\kappa_b(\xi) = \xi^\lambda$. The moment operation can be applied to Eq. 3 to give the dimensionless moment equations (Madras and McCoy, 2002) for integer values of j, as follows

$$dP^{(j)}/d\theta = -P^{(j+\lambda)} + 2(1 + j)^{-1}P^{(j+\lambda)} - 2\gamma P^{(j)}P^{(0)}$$
$$+ \gamma\sum_{d=0}^{j}\binom{j}{d}P^{(j-d)}P^{(d)} \tag{7}$$

where $\binom{j}{d}$ is the binomial coefficient. The moment equations are obtained by substituting $j = 0$, 1, and 2 in Eq. 7

$$dP^{(0)}/d\theta = P^{(\lambda)} - \gamma P^{(0)2} \tag{8}$$

$$dP^{(1)}/d\theta = 0 \tag{9}$$

$$dP^{(2)}/d\theta = -(1/3)P^{(2+\lambda)} + 2\gamma P^{(1)2} \tag{10}$$

Mass conservation, $P^{(1)}(\theta) = P_0^{(1)} = 1$, is ensured by Eq. 9.

McCoy and Madras (1998, 2002, 2003b) showed that when $\lambda = 1$, any initial distribution evolves to the exact self-similar exponential solution in terms of the average element mass, $P^{avg}(\theta)$

$$P(\xi, \theta) = [P^{avg}(\theta)]^{-2}\exp[-\xi/P^{avg}(\theta)] \tag{11}$$

whose moments are simply

$$P^{(\nu)} = (P^{avg})^{\nu-1}\Gamma(\nu + 1) \tag{12}$$

The similarity variable $\xi/P^{avg}(\theta)$ in Eq. 11 combines scaled mass ξ and time θ. The distribution is thus governed by $P^{avg}(\theta)$, which satisfies the differential equation

$$dP^{avg}/d\theta = -(P^{avg})^2 + \gamma \tag{13}$$

For an exponential initial distribution with $P^{avg}(\theta = 0) = P_0^{(1)}/P_0^{(0)} = 1$, the solution to Eq. 13 has been reported (McCoy and Madras, 1998, 2002)

$$P^{avg}(\theta) = \gamma^{1/2}\tanh[\theta\gamma^{1/2} + \tanh^{-1}(1/\gamma^{1/2})] \tag{14}$$

We wish to incorporate as a parameter in the theory the dispersed fluid volume per vessel volume, α. If the elements are spherical of radius r, then the fluid-element area/volume is $3/r = 3(3x/4\pi\rho)^{-1/3} = gx^{-1/3}$, in terms of $g = (4\pi\rho/9)^{1/2}$ and the total dispersed-fluid area per vessel volume for elements in the range $(x, x + dx)$ is $\alpha g x^{-1/3}\, p(x, t)dx$. Of course, the fluid elements will not be exactly spherical for turbulent mixing, and the coefficients of x^ν may be different from the expressions above. For example, let us consider that fragmentation occurs by stretching cylindrical fluid elements of radius $r(t)$ and then severing them into two random segments of area/volume = $2/r$. The cylinder mass in terms of its length z is $x = \pi r^2 z\rho$, from which we find the total element area per vessel volume proportional to $\alpha g x^{-1/2}$, where $g = (\pi z\rho)^{1/2}$. If fragmentation occurs by stretching flat slabs and then cutting them into two slabs, and if the ribbonlike slabs, or striations, are thin of thickness y and surface $2S$, then edge areas can be neglected and the element area per element volume is $2/y$. In terms of the element mass $x = Sy\rho$, the element area per vessel volume is

proportional to $\alpha g x^{-1}$ with $g = 2S\rho$. Although in this case the moment with $\nu = -1$ in Eq. 6 diverges, we can compute the moment for ν arbitrarily close to -1. These arguments, indicating $\nu = -1/3$, $-1/2$, and near -1 for the spherical, cylindrical, and slab geometries, respectively, suggest that a low-order negative moment of $p(x, t)$ governs the kinetics of a reactive mixing system. This is particularly significant considering that the negative moments increase strongly when fragmentation dominates the mixing process.

Reaction Kinetics I

Parallel-competitive reactions (I)

In the present project we focus on competitive reactions previously used to study turbulent mixing in batch reactors. Bourne and Yu (1994) examined reactions that compete for the reactant A

$$A + B \overset{k_1}{\rightarrow} P \tag{15}$$

$$A + C \overset{k_2}{\rightarrow} Q \tag{16}$$

For reactions 15 and 16, the reactant A can be in the dispersed phase and B and C in the continuous phase, or vice versa. For the usual well-stirred batch kinetics, if $k_2 \ll k_1$, then the final yield of Q will be negligible relative to the yield of P. If $k_2 \approx k_1$, then the yield of Q will be comparable to the yield of P. We will see that the Damkohler number defined below has the same behavior as these rate constants. When the rate coefficient k_1 is orders of magnitude larger than k_2 (Baldyga and Bourne, 1999), its rate is diffusion limited; thus, A and B react at the interface as fast as they can diffuse together. Consistent with the assumption that the dispersed fluid elements have uniform concentration, the diffusion of B to the interface in the continuous fluid controls the rate. This suggests using a rate expression with a coefficient of the order of the diffusivity of B, thus $k_m \sim D/\delta^2$, in terms of a boundary layer thickness δ. Because the reactant vanishes when it reaches the interface, the concentration driving force has only the bulk value and the rate is thus first-order in the concentration of B. Given the volume fraction α of the added solution with reactant A, the rate is proportional to the surface area per unit volume of a fluid element (i.e., to x^{ν}), where as explained above, $0 \geq \nu > -1$.

We consider a batch operation so that no flow enters or leaves the vessel. The generalization to a continuous-flow stirred tank is straightforward and provides analogous results. The time-dependent yields of P and Q will depend on the rate constants, and in particular the ratio k_2/k_m, initial concentrations, and surface area between the continuous and dispersed phases. The surface area is determined by the degree of mixing, which depends on fragmentation and coalescence parameters, λ and γ, respectively. The reaction of A and B can be represented as an integral over the distribution of fluid elements, $p(x, t)$. Reaction 16 is first-order in each concentration, or second-order overall (Bourne and Yu, 1994; Li and Toor, 1986). We consider A as the limiting reactant, so we must account for total moles of A reacted. If α and $1 - \alpha$ are the dispersed- and continuous-fluid volume fractions, respectively, then

$$\alpha dc_A/dt = (1 - \alpha)(dc_B/dt + dc_C/dt) \tag{17}$$

For the continuous phase concentrations, the rate expressions are

$$dc_P/dt = -dc_B/dt = k_m c_B(t)\, g\alpha p^{(\nu)}(t) \tag{18}$$

$$dc_Q/dt = -dc_C/dt = k_2 c_A(t) c_C(t)\, g\alpha p^{(\nu)}(t) \tag{19}$$

where the moment $p^{(\nu)}(t)$ is defined by Eq. 2. Initial conditions are $c_A(t = 0) = c_{A0}$, $c_B(t = 0) = c_{B0}$, $c_C(t = 0) = c_{C0}$, and $c_P(t = 0) = c_Q(t = 0) = 0$.

We can write the dimensionless mass balances in terms of concentrations scaled by the initial concentration, c_{A0}, of the limiting reactant A

$$C_A = c_A/c_{A0}, \quad C_B = c_B/c_{A0}, \quad C_C = c_C/c_{A0}, \quad C_P = c_P/c_{A0}, \quad C_Q = c_Q/c_{A0} \tag{20}$$

and define the rate constants,

$$\kappa_m = k_m g p_0^{(0)} (p_0^{avg})^{\nu}/k_{bo} \quad \text{and} \quad \kappa_2 = k_2 g p_0^{(0)} (p_0^{avg})^{\nu} c_{A0}/k_{bo} \tag{21}$$

The parameters κ_m and κ_2 are the ratios of reaction rates to breakage rate, and incorporate both chemical kinetics and geometry of the element. This reveals how mixing alters the reactions rates by including the effects of turbulence into κ_m and κ_2. If we assume $k_m = D/\delta^2$ for a diffusion-controlled rate over a characteristic distance δ, then the ratio κ_2/κ_m is a Damkohler number of the typical form (Baldyga and Bourne, 1999):

$$\kappa = \kappa_2/\kappa_m = k_2 c_{A0} \delta^2/D \tag{22}$$

where we note that the moments in Eq. 21 have canceled. Increased mixing intensity will decrease δ, so κ depends on the hydrodynamic state, and in particular on the Reynolds number. As in other reactive mixing models, for example, the engulfment model (Baldyga and Bourne, 1999; Bourne and Yu, 1994), the Damkohler number can be related to the energy dissipation rate, and hence to power input and geometry of the mixer.

The dimensionless equations corresponding to Eqs. 17–19 are

$$\alpha dC_A/d\theta = (1 - \alpha)(dC_B/d\theta + dC_C/d\theta) \tag{23}$$

$$dC_B/d\theta = -\kappa_m \alpha C_B P^{(\nu)}(\theta) = -dC_P/d\theta \tag{24}$$

$$dC_C/d\theta = -\kappa_2 \alpha C_A C_C P^{(\nu)}(\theta) = -dC_Q/d\theta \tag{25}$$

with initial conditions,

$$C_A(\theta = 0) = 1, \quad C_B(\theta = 0) = C_{B0}, \quad C_C(\theta = 0) = C_{C0}, \quad C_P(\theta = 0) = C_Q(\theta = 0) = 0 \tag{26}$$

Because A is the limiting reactant, we require that initial moles of B and C are greater than initial moles of A, thus, both C_{C0} and $C_{B0} \geq \alpha/(1 - \alpha)$ must be true. According to Eq. 25, when A is exhausted at time $\theta = \theta_f$, $C_A(\theta_f) = 0$, and C_C reaches its minimum value, C_{Cf}. Once the population balance has been solved for $P(\xi, \theta)$, the moment expression can be evaluated and substituted into the rate equations for evaluation of time-dependent concentrations. In the perfectly segregated case, the elements maintain their integrity so that the fluid elements do not change their size distribution; thus $P^{(\nu)}(\theta) = P^{(\nu)}(0)$. In the perfect mixing case the dispersed phase is instantaneously and totally disintegrated to a molecular level and $P^{(\nu)}(\theta)$ immediately reaches a large constant value.

The dimensionless product yields, or fractional conversions, relative to the limiting reactant A are defined as (Bourne and Yu, 1994) $X_P = C_{Pf}/(C_{Pf} + C_{Qf})$ and $X_Q = C_{Qf}/(C_{Pf} + C_{Qf})$, ensuring that values are in the interval [0, 1]. According to Eqs. 23–25, $(1 - \alpha)(C_P + C_Q) = \alpha(1 - C_A)$, and thus with $C_{Af} = 0$ we have

$$X_P = (C_{B0} - C_{Bf})(1 - \alpha)/\alpha \quad \text{and}$$
$$X_Q = (C_{C0} - C_{Cf})(1 - \alpha)/\alpha = 1 - X_P \quad (27)$$

Because the rate of reaction 16 is slow relative to reaction 15, the competition between the reactions will favor reaction 15. This effect is enhanced for larger surface areas between the two phases, so that for perfect mixing ($\kappa \ll 1$) the yield of Q vanishes, $X_Q \rightarrow 0$. Because κ_2 is a ratio of reaction rate to breakage rate, decreasing κ_2 implies more efficient fragmentation and more turbulence. At the other extreme, for total segregation and a very slow reaction 1 ($\kappa \gg 1$), only Q would be produced, $X_Q \rightarrow 1$. All cases between perfect mixing and segregation will exhibit intermediate yields. The effects of the dimensionless rate coefficients, κ_m and κ_2, on yield are thus conspicuously like the effects of usual rate constants in a well-stirred batch reactor.

Applying the transformation for the temporal variable,

$$d\tau = \kappa_m P^{(\nu)}(\theta)d\theta \quad \text{or} \quad \tau = \kappa_m \int_0^\theta P^{(\nu)}(\theta)d\theta \quad (28)$$

to Eqs. 23–25 reduces the kinetics to the simple batch stirred-tank reactor

$$\alpha dC_A/d\tau = (1 - \alpha)(dC_B/d\tau + dC_C/d\tau) \quad (29)$$

$$dC_B/d\tau = -\alpha C_B = -dC_P/d\tau \quad (30)$$

$$dC_C/d\tau = -\kappa\alpha C_A C_C = -dC_Q/d\tau \quad (31)$$

and substantially reduces the mathematical complexity. For the special case $\nu = 1$, $P^{(\nu)}$ is constant and $\tau = k_m\theta P^{(1)}$. The nonlinear differential equations depend only on the Damkohler number κ, the volume ratio α, and the initial conditions C_{C0} and C_{B0}, and are readily solved numerically. It is interesting that the equations are compatible with the well-stirred batch reactor model, but in terms of the compressed time variable τ.

The component B (Eq. 30) decreases exponentially with τ,

$$C_B(\tau) = C_{B0}\exp(-\alpha\tau) \quad (32)$$

When Eq. 31 is subtracted from Eq. 29, and Eq. 32 is used to eliminate $C_B(\tau)$, one finds a differential equation for the difference $u(\tau) = C_A\alpha/(1 - \alpha) - C_C$

$$du/d\tau = -\kappa(u - b_o) \quad (33)$$

where $b_o = \alpha/(1 - \alpha) - C_{B0} - C_{C0}$. The equation is easily integrated with the initial condition $u(0) = \alpha/(1 - \alpha) - C_{C0}$, and the solution is

$$C_A(\tau)\alpha/(1 - \alpha) - C_C(\tau) = C_{B0}\exp(-\kappa\alpha\tau) + \alpha/(1 - \alpha) - C_{B0} - C_{C0} \quad (34)$$

The reaction ends when the reactant A is depleted, $C_A(\tau = \tau_f) = 0$, which defines the final time, τ_f, at which C_C has reached its maximum, asymptotic value

$$C_{Cf} = C_{B0}[1 - \exp(-\alpha\tau_f)] + C_{C0} - \alpha/(1 - \alpha) \quad (35)$$

This can be used to calculate the final yield, X_Q, from Eq. 27. Equation 34 can also be used to eliminate $C_A(\tau)$ from Eq. 31, which yields

$$dC_C/d\tau = -\kappa C_C\{C_C(\tau) - C_{C0} + \alpha/(1 - \alpha) + C_{B0}[\exp(-\alpha\tau) - 1]\}(1 - \alpha) \quad (36)$$

This nonlinear differential equation is easily solved numerically to determine the dynamic state of the system at any time. We applied the software Mathematica™, which solves the system in seconds. Interestingly, Mathematica finds an analytical solution to Eq. 36 for the approximation, $e^{-\alpha\tau} \approx 1 - \alpha\tau$. For the common case $\alpha = 1 - \alpha = 0.5$ and $C_{C0} = C_{B0} = 1$, the solution is remarkably simple

$$C_C(\tau) = \exp(\kappa\tau^2/8)/[1 + (\kappa\pi/2)^{1/2}\text{erf } i(\tau\kappa^{1/2}/2^{3/2})] \quad (37)$$

in terms of erf $i(z) = \text{erf}(iz)/i$.

A key result of the analysis above is that the final conversion fractions, $X_P = 1 - X_Q$, depend on the Damkohler number κ, the volume ratio α, and the initial conditions, C_{C0} and C_{B0}, but not on ν. The time dependency for reactive mixing can be represented by plots of C_C and of C_A vs. τ, which increases with $\theta = tk_{bo}$. In accord with the recommendation by Baldyga and Bourne (1999), the effect of the volume ratio α is explicit. The final conversion as a function of the Damkohler number κ for different values of the initial conditions, C_{C0} and C_{B0}, is also a key result.

Reaction Kinetics II

Series-parallel reactions (II)

The two series-parallel (competitive-consecutive) reactions with separate feeds of A and B (Baldyga and Bourne, 1999;

Levenspiel, 1999; Li and Toor, 1986) have also played a significant role in reactive mixing research

$$A + B \xrightarrow{k_1} R \tag{38}$$

$$A + R \xrightarrow{k_2} Q \tag{39}$$

Similar to Reaction I, if the rate of reaction 38 is much faster than that of reaction 39, it is mass-transfer controlled with rate coefficient k_m. As above, the reaction of A and B at the interface can be represented as an integral over the distribution, $p(x, t)$, to account for the interfacial area where reaction occurs. Consistent with reactions written as Eqs. 38 and 39, concentrations are scaled with the limiting-reactant initial concentration, c_{A0}. The dimensionless rate expressions for the continuous fluid that contains reactant B are

$$dC_B/d\theta = -\kappa_m \alpha C_B P^{(\nu)}(\theta) \tag{40}$$

$$dC_Q/d\theta = \kappa_2 \alpha C_A C_R P^{(\nu)}(\theta) \tag{41}$$

$$dC_R/d\theta = \alpha(\kappa_m C_B - \kappa_2 C_A C_R) P^{(\nu)}(\theta) \tag{42}$$

and for the dispersed fluid containing A

$$dC_A/d\theta = -(1 - \alpha)(\kappa_m C_B + \kappa_2 C_A C_R) P^{(\nu)}(\theta) \tag{43}$$

Initial conditions are $C_A(t = 0) = 1$, $C_B(t = 0) = C_{B0}$, and $C_R(t = 0) = C_Q(t = 0) = 0$. These conditions for B and the limiting reactant A require that $C_{B0} \geq \alpha/(1 - \alpha)$. The concentrations C_A and C_B are average concentrations over the fluid elements. Fragmentation will yield two elements of identical concentration if the concentration is uniform within the dispersed elements, as we have assumed. The approximation is less accurate for coalescence between two elements having quite different concentrations (McCoy and Madras, 2003a), but coalescence has little influence on reactive turbulence, which is primarily dispersive.

For a batch operation, when A is the reactant in the dispersed fluid elements and B, R, and Q are present in the continuous-fluid elements, the yield will depend on the Damkohler number, Eq. 22. Li and Toor (1986) show an empirical relationship between D/δ^2 and Reynolds number for jets in tubular flow reactors. The two limits of mixing are perfect segregation and perfect mixing. For instantaneous perfect mixing ($\kappa \ll 1$), reactant A is consumed completely by the first reaction and the yield of the second reaction is negligible. If molecular-scale mixing is not attained, however, A is not exhausted by the first reaction and thus can react with R. The yield of Q increases as κ increases.

The transformation 28 simplifies the dynamic equations

$$dC_B/d\tau = -\alpha C_B \tag{44}$$

$$dC_A/d\tau = -(1 - \alpha)[C_B + \kappa C_A C_R] \tag{45}$$

$$dC_R/d\tau = \alpha[C_B - \kappa C_A C_R] \tag{46}$$

$$dC_Q/d\tau = \kappa \alpha C_A C_R \tag{47}$$

Again, with the compressed time variable τ, we find the model satisfies differential equations for the well-stirred batch reactor. Equation 44 has the exponential solution, Eq. 32, which allows C_B to be eliminated from Eqs. 45 and 46. The two resulting nonlinear differential equations can be solved routinely and without difficulty. Alternatively, when one subtracts Eq. 45 from Eq. 46, and then substitutes Eq. 32, the resulting differential equation can be solved immediately for $C_{A0} = 1$, as follows

$$C_R(\tau) + [1 - C_A(\tau)]\alpha/(1 - \alpha) = 2C_{B0}[1 - \exp(-\alpha\tau)] \tag{48}$$

Equation 48 gives the final conversion fraction X_R when C_A falls to zero. The fractional conversions

$$X_Q = C_{Qf}/(C_{Qf} + C_{Rf}) \quad \text{and} \quad X_R = C_{Rf}/(C_{Qf} + C_{Rf}) = 1 - X_Q \tag{49}$$

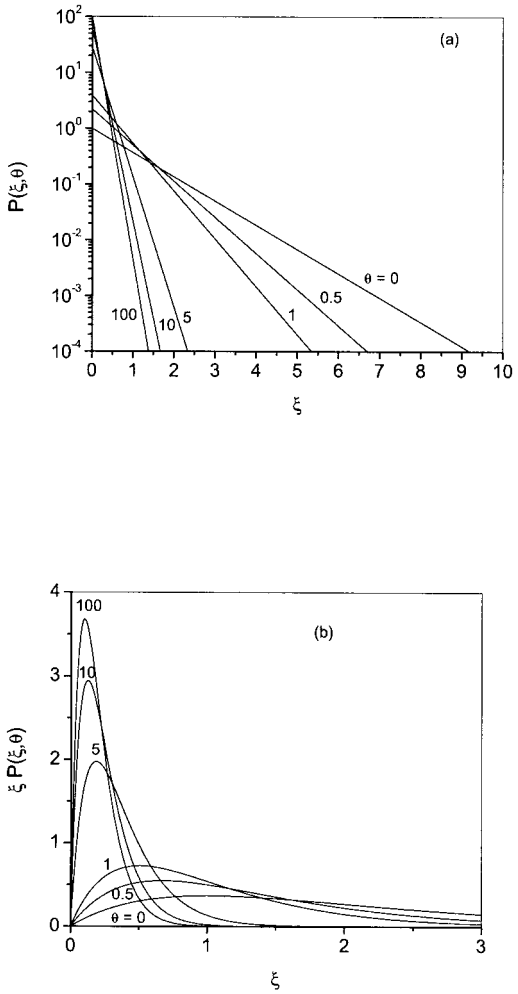

Figure 1. Time dependency of the fluid element size distribution, (a) $P(\xi, \theta)$, and (b) $\xi P(\xi, \theta)$, for $\lambda = 1$, $\gamma = 0.01$, and an exponential initial condition with $P^{avg}(\theta = 0) = 1$.

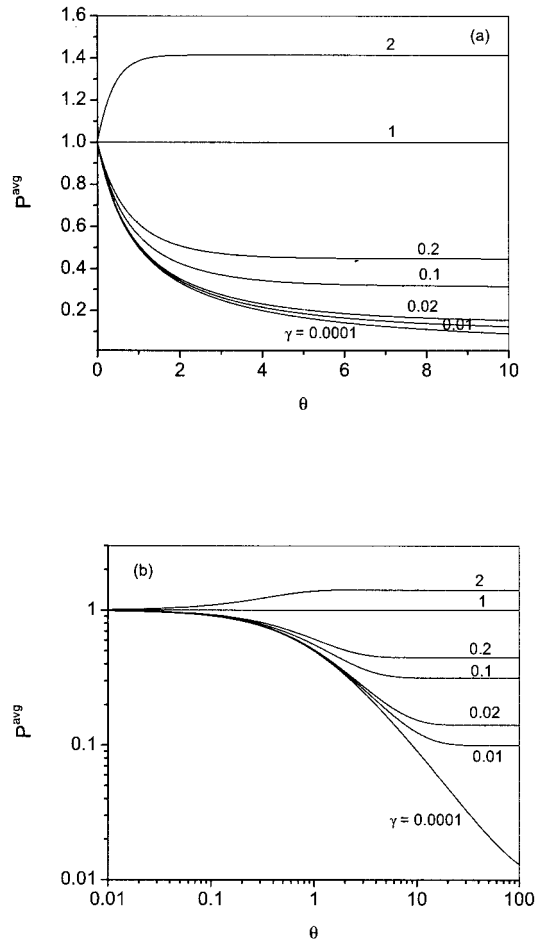

Figure 2. Time evolution of $P^{avg}(\theta)$ from an exponential initial condition with $P^{avg}(\theta = 0) = 1$ for $\lambda = 1$ and various γ on (a) linear and (b) log coordinates.

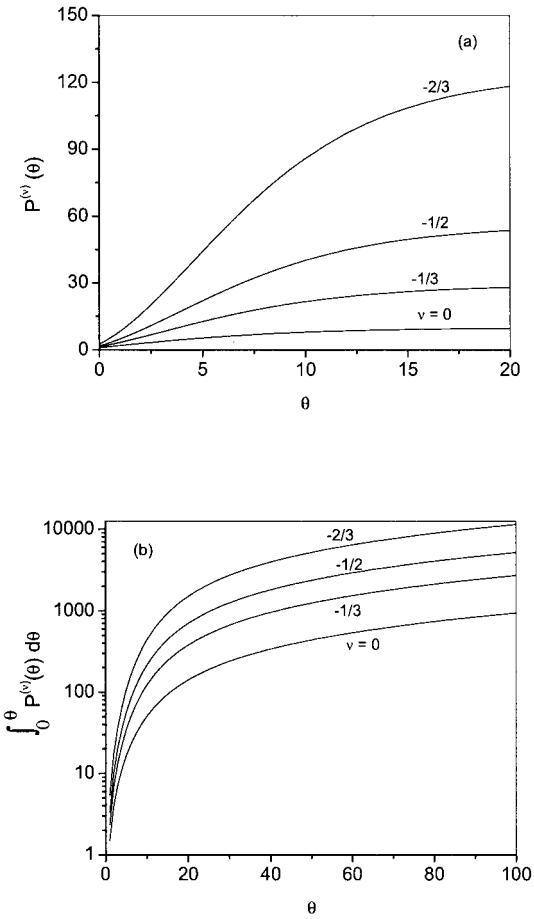

Figure 3. Time evolution of the (a) moments, $P^{(\nu)}(\theta)$, and (b) the moment integrals, $\int_0^\theta P^{(\nu)}(\theta)d\theta$, from an exponential initial condition with $P^{avg}(\theta = 0) = 1$ for $\lambda = 1$, $\gamma = 0.01$, and $\nu = 0, -1/3, -1/2$, and $-2/3$.

can be evaluated by solving for C_{Qf} or C_{Rf}, and then noting that by combining Eqs. 46, 48, and 32, one obtains

$$C_{Qf} + C_{Rf} = C_{B0}[1 - \exp(-\alpha\tau_f)] \tag{50}$$

where the subscript f indicates the final state when the limiting reactant A has been exhausted. We conclude that final conversion can be computed for any value of κ, α, and C_{B0} when τ_f is known. The time τ_f, but not X_Q, depends on the parameter ν. For the time dependency of the reactants, Eq. 48 can be used to eliminate $C_A(\tau)$ from Eq. 46, which yields

$$dC_R/d\tau = \alpha C_{B0}e^{-\alpha\tau} + \kappa\alpha C_R \times [-1 - \{C_R - 2C_{B0}(1 - e^{-\alpha\tau})\}(1 - \alpha)/\alpha] \tag{51}$$

Easily evaluated numerically, the time series depends only on the parameter κ, the volume ratio α, and the initial condition C_{B0}. An analytical solution to Eq. 51 in terms of hypergeometric functions and Hermite polynomials is found by Mathematica, but is too complicated for straightforward evaluation. With appropriate software, one usually prefers the simplicity of a numerical solution for such ordinary differential equations.

Results and Discussion

Given that our computations are for a batch system, Eq. 9 ensures that total mass is invariant in time, $P^{(1)}(\theta) = P_0^{(1)} = 1$. The rate coefficient for coalescence is considered independent of x, but the rate coefficient for fragmentation increases with element size as x^λ. As we have indicated, for $\lambda = 1$ the dispersed-fluid elements evolve according to an exact similarity solution. For values of λ other than zero and unity, numerical methods have to be used to solve the PBE and determine the time evolution of the PSD. Equation 13 gives the time evolution of the average size of the elements when $\lambda = 1$. The time dependency of the size distribution for dispersed-fluid elements (Eq. 11) is shown plotted two different ways. In Figure 1(a) the exponential similarity solution ($\lambda = 1$) decreases in mass when fragmentation dominates ($\gamma = 0.01$). Turbulent reactive mixing is characterized by strong shearing of the dispersed reactant phase, so that the ratio γ of aggregation to fragmentation rates is a small number. The scaled mass distribution $\xi P(\xi, \theta)$ represents the mass per vessel volume in

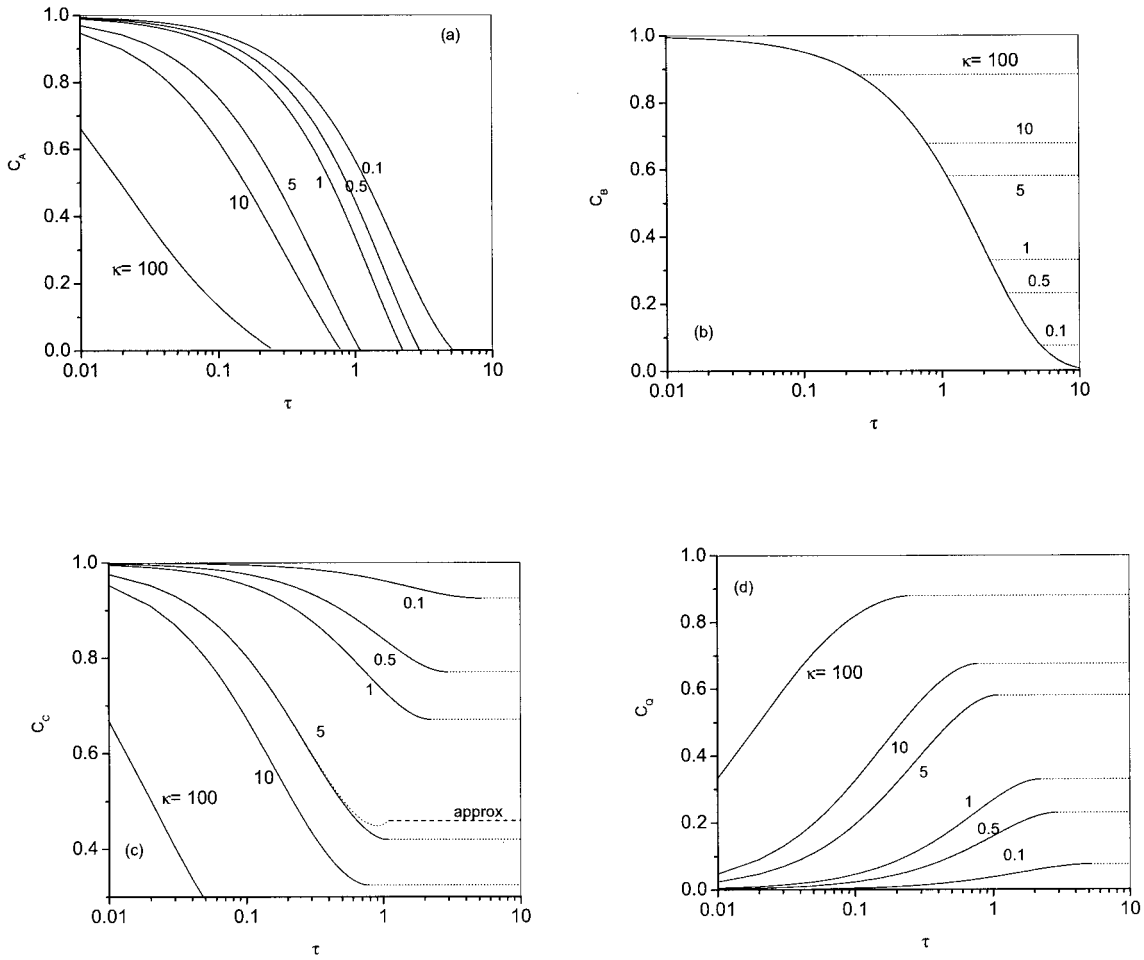

Figure 4. Evolution of the scaled concentrations C_A, C_B, C_C, and C_Q with compressed time τ for various κ (Reaction I) and $\alpha = 0.5$.

The initial concentrations are $C_{A0} = C_{B0} = C_{C0} = 1$ and $C_{Q0} = 0$. The horizontal dotted lines indicate the final concentrations when the limiting reactant A is depleted. The dashed line is an approximation (for $\alpha\tau < 1$) to the solution.

the range (ξ, $\xi + d\xi$), and decreases to smaller sizes with time [Figure 1(b)]. The dimensionless average mass as a function of time is displayed in Figure 2 for several values of γ, which decreases as agglomeration is dominated by breakage. If γ is less than unity, degradation dominates, and if γ is greater than unity, coalescence plays the dominant role. For reactive mixing, efficient fragmentation is the desired behavior, so small values of γ are essential.

A comparison of moments $P^{(\nu)}(\theta)$ with $\nu = 0, -1/3, -1/2$, and $-2/3$ is shown in Figure 3a for $\gamma = 0.01$ and $\lambda = 1$. For this case of dominant fragmentation the negative-order moments are larger than the positive-order moments, and the difference increases nonlinearly with time. In Figure 3b plots of the compressed time variable τ/k_m (Eq. 28) reveal the strong nonlinearity imposed by the turbulence model.

For Reaction I, Figure 4 shows the time evolution of the concentrations C_A, C_B and C_C for several values of the rate ratio, κ, or Damkohler number. As determined in other models of reactive mixing, this ratio plays a critical role in determining the time dependency of the concentrations. Because the component A is the limiting reactant, C_A vanishes [Figure 4a] after a definite time τ_f. The concentration of B decreases exponentially independently of κ (Eq. 32) and ceases reaction when A is depleted [Figure 4b]. Concentrations after the reaction stops are shown as dotted horizontal lines. The concentration of C reaches a minimum (Eq. 31) when A vanishes, and is shown remaining constant afterward [Figure 4c]. The approximate analytical solution (Eq. 37), valid only for $\alpha\tau < 1$, is drawn as a dashed line for $\kappa = 5$. The product Q increases with time to its maximum (Eq. 31) at τ_f [Figure 4d].

Figure 5 shows how the final conversion X_Q for Reaction I depends on κ for (a) different initial concentrations of B, (b) different initial concentrations of C, and different volume fractions α. The Damkohler number κ depends on the length scale δ, so the similar shape of the curves makes it clear that shifting the value of κ would allow the data to match the model curves satisfactorily. The effect of the volume fraction α, or volume ratio $\alpha/(1 - \alpha)$, on conversion, according to the model and corroborated by experiments (Figure 10 of Bourne and Yu, 1994), is relatively weak [Figure 5c]. The trend of increasing conversion for $X_Q < 0.45$ with increased volume fraction is consistent with experimental observations and with predictions of the engulfment model (Baldyga and Bourne, 1999, p. 589). The IEM model, however, predicts an opposite trend, in addi-

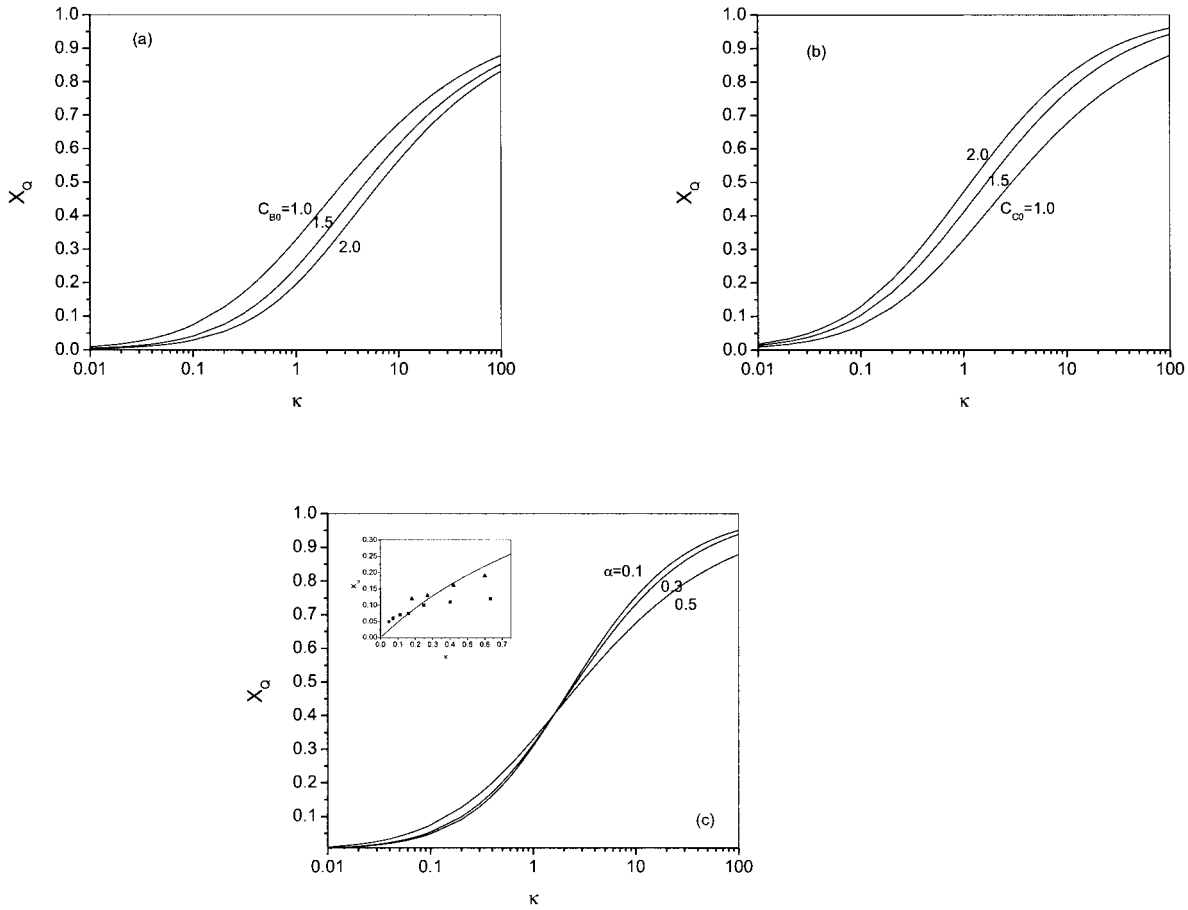

Figure 5. Variation of fractional conversion X_Q with kappa for (a) $C_{C0} = 1$, $\alpha = 0.5$, and various C_{B0}, (b) $C_{B0} = 1$, $\alpha = 0.5$, and various C_{C0}, (c) $C_{B0} = C_{C0} = 1$ and $\alpha = 0.1, 0.3, 0.5$.

The inset of (c) shows the prediction of the model (line) and the experimental data (discrete points) with $C_{B0} = C_{C0} = 0.2$ and $\alpha = 0.02$ of Baldyga and Bourne (1999).

tion to an X_Q asymptote less than unity, and is therefore questionable (Baldyga and Bourne, 1999, p. 590). The current model shows the curves crossing and a reversed trend for fractional conversions not usually realized experimentally (that is, above 0.45). The inset of Figure 5c shows the variation of the final conversion X_Q with κ for $C_{B0} = C_{C0} = 0.2$ and $\alpha = 0.02$. The discrete points represent two different sets of experimental data reported by Baldyga and Bourne (1999). These experimental points are multiplied by a constant such that they nearly collapse onto a single curve predicted by the model. The model predictions are higher than the data at larger Damkohler number. Other models (Baldyga and Bourne, 1999) likewise overestimate these data. It is possible that as the impeller speed is increased to raise κ, the turbulent state is altered in a nonuniform way throughout the vessel, thus changing the time dependency of $P^{(\nu)}$ and the time for depletion of limiting reactant A.

For Reaction II, Figure 6 shows the compressed time (τ) dependency of the concentrations C_A, C_B, C_R, and C_Q for several values of the ratio κ. The limiting reactant is A, which vanishes at time τ_f [Figure 6a]. The reactant B is independent of κ and decreases exponentially until the time τ_f [Figure 6b]. Product R increases with time until A is depleted [Figure 4c]. Product Q also increases with time, and according to Eq. 47, reaches its maximum at time τ_f [Figure 4d].

Figure 7 displays graphs of the final conversion for Q vs. κ depending on the initial condition C_{B0} [Figure 7a] and on the volume fraction α [Figure 7b]. Because of the uncomplicated linear dependency of the coefficients κ and α in Eqs. 44–47, the curves have similar, conformal shapes. This ensures that the experimental data of Li and Toor (1986) for conversion vs. Damkohler number will fit the model if a single factor is chosen to multiply κ. The factor can be determined for only a single datum, so curve fitting is not necessary. The experiments were for jet streams of reactant dispersed into continuously-flowing second reactant. When inlet concentrations and flow rates are equal ($C_{A0} = C_{B0} = 1$ and $\alpha = 0.5$), the symmetry of Eqs. 44–47 indicates that yields are independent of whether reactant A is in the dispersed or continuous phase. This result was reported by Li and Toor (1986), who performed the jet experiments with either A or B in the dispersed phase and found that the yield was similar to within a few percent. The discrete points in Figure 7(a) and (b) represent the experimental data of Li and Toor (1986) for $C_{B0} = 1.0$ and $\alpha = 0.5$. A single factor (=2/15) is chosen to multiply κ of the experimental data to fit the model.

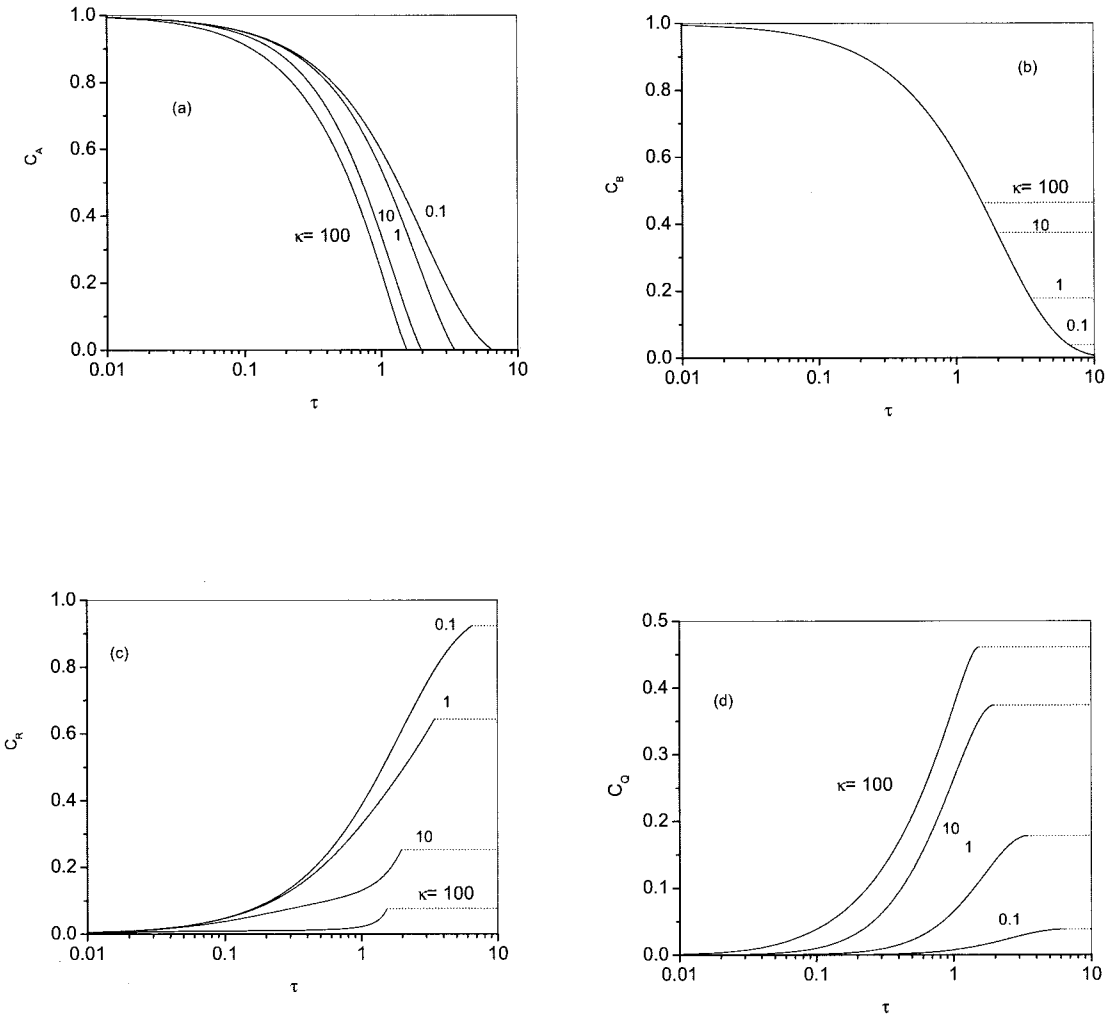

Figure 6. Evolution of the scaled concentrations C_A, C_B, C_R, and C_Q with compressed time τ for various κ (Reaction II) and $\alpha = 0.5$.

The initial conditions are $C_{A0} = C_{B0} = 1$ and $C_{Q0} = C_{R0} = 0$. The horizontal dotted lines indicate the final concentrations when the limiting reactant A is depleted.

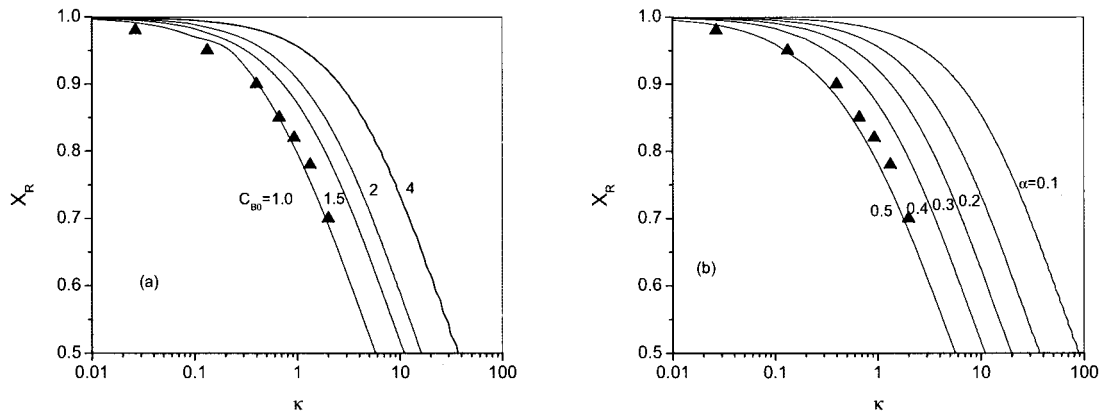

Figure 7. Variation of fractional conversion X_R with κ (Reaction II) for (a) $\alpha = 0.5$ and various C_{B0}, (b) $C_{B0} = 1$ and various α.

The other parameters are $C_{A0} = 1$ and $C_{R0} = C_{Q0} = 0$. Discrete points are experimental data for $C_{B0} = 1.0$ and $\alpha = 0.5$ of Li and Toor (1986).

The analysis and discussion above reveals that two kinds of results for competitive reactions can be examined, either experimentally or theoretically, in reactive mixing. One is the time dependency of the concentrations, which is straightforward to compute with the current model but may be difficult to measure in an experiment. More accessible is the dependency of the final yield on the Damkohler number, volume fraction, and initial conditions. This is the key result essential to a realistic mathematical model and usually measured in experiments on reactive mixing. Most models that postulate a fast, diffusion-controlled reaction competing with a slow, second-order reaction have adequately produced this critical result, although perhaps not as readily as the current model. The present theory shows that if the chemical kinetics are correctly represented, then the turbulent mixing acts to fragment the dispersed reactant and compress (or stretch) the time variable. The final time for computing the yield is when the limiting reactant is depleted, and is conditional on the ratio of rate coefficients (the Damkohler number). With the understanding that reaction occurs at the evolving interface of dispersed and continuous fluids, no impediments hinder the application of the model to other reaction mechanisms. Furthermore, the computations will be straightforward numerical solutions of nonlinear differential equations.

Conclusions

The novel reactive mixing model we have proposed is based on an approach to turbulence involving cascading fragmentation of fluid elements in a stirred batch reactor. A population dynamics equation governs the evolution of the hierarchy of fluid-element sizes and intrinsically conserves mass. An exact solution of this equation gives the time evolution of the mass distribution function, but does not prescribe the element shape. This fluid-element shape determines the contact surface area between the elements and the continuous fluid and thus the chemical reaction among reactants. Different shapes yield different powers of mass to represent the interfacial influence on reaction rate. An averaging operation over the size distribution yields negative moments varying with time. For competitive reactions the kinetic expressions can be transformed to equations familiar as stirred-tank reactions by defining a compressed time in terms of the negative moment of the fluid element size distribution.

Several features of the current model facilitate evaluation such that computations are straightforward and quick. Although mastery of distribution kinetics by using population balance equations requires a significant effort, the same framework is applicable to a range of chemical engineering processes. The analytical and closed-form self-similar solution to the population dynamics equation for dispersed-fluid breakup allows ready evaluation of the negative moments governing the interfacial area/volume. This allows the dispersed fluid volume fraction effect to be explicit. The reactions occur at this interfacial region where reactants come in contact with each other. We have assumed that the fast reaction is first-order diffusion-influenced and the slow reaction is second-order in reactants. The fast reaction is controlled by diffusion in the continuous fluid while reactant concentration in the dispersed fluid is uniform, for example, in thin, ribbon-like dispersed elements. This assumption should increase in validity for all smaller dispersed elements where concentration inhomogeneities are more rapidly smoothed by diffusion. Although we have chosen the analytic self-similar exponential distribution to illustrate the logical development and major implications of the model, other choices for the mass dependency of fragmentation and coalescence rate coefficients, k_b and k_a, will yield other kinds of size distributions.

Our goal has been to base the current model on familiar chemical engineering concepts and parameters. The model meets the standard of fully incorporating the essential parameters: initial reactant concentrations (c_{A0}, c_{B0}, c_{C0}), volume ratio of added (dispersed) fluid (α), reaction rate coefficient for the slow reaction (k_2), diffusion-influenced rate of the fast reaction (k_m), and parameters for turbulent fragmentation (k_{bo} and γ). We have shown how a nonlinear time-variable transformation that includes the turbulent-fragmentation effect reduces the differential equations to the simple stirred-tank model. This transformation provides new insights into reactive mixing by aggregating turbulence structure into the temporal variable. Thus the fluid dynamical details are less critical than the essential features of turbulence, namely, randomness, eddy viscosity, cascading, and scaling. To fit experimental data, all reactive-mixing models incorporate parameters that typically are empirical and cannot be estimated from fundamental concepts. The model can be evaluated with relatively straightforward computations. A single experimental point allows matching of our theory and experiment for fractional conversion vs. Damkohler number. The results and conclusions suggest that a minimal theory accounting for essential phenomena can realistically represent turbulent reactive mixing sufficiently well for many applications.

Notation

k_a = rate coefficient for aggregation (coalescence)
k_b = rate coefficient for fragmentation (breakage)
k_1 = rate coefficient for reactions 15 and 38
k_2 = rate coefficient for reactions 16 and 39
C = concentration scaled by the initial concentration of the limiting reactant, A
X = fractional conversion (Eqs. 27 and 49)

Greek letters

α = dispersed fluid volume fraction
ρ = mass density
δ = fluid element or boundary layer thickness
$\Omega(x, x')$ = fragmentation kernel
λ = exponent of the breakage rate coefficient
τ = compressed time defined by Eq. 28
θ = dimensionless time (Eq. 4)
κ_m = dimensionless rate coefficient (Eq. 21)
κ_2 = rate coefficient (Eq. 21), representing the ratio of reaction rate to breakage rate
κ = Damkohler number, defined in Eq. 22
γ = dimensionless rate coefficient for coalescence
ξ = dimensionless mass
(ν) = superscript indicating νth mass moment

Subscripts

A = limiting reactant A
B = reactant B
C = reactant C
Q = product Q
R = product R
0 = initial condition

Literature Cited

Baldyga, J., and J. R. Bourne, *Turbulent Mixing and Chemical Reactions*, Wiley, Chichester, U.K. (1999).

Başağaoğlu, H., T. R. Ginn, C. T. Green, and B. J. McCoy. "Modeling Transport in Heterogeneous Media: Tracer Dynamics in Complex Flow Networks," *AIChE J.*, **48**, 1122 (2002).

Bourne, J. R., and S. Yu, "Investigation of Micromixing in Stirred Tank Reactors Using Parallel Reactions," *Ind. Eng. Chem. Res.* **33**, 41 (1994).

Chakroborty, S., and V. Balakotaiah, "Two-Mode Models for Describing Mixing Effects in Homogeneous Reactors," *AIChE J.*, **48**, 2571 (2002).

Curl, R. L., "Dispersed Phase Mixing—Theory and Effects in Simple Reactors," *AIChE J.*, **9**, 175 (1963).

Dutta, A., and J. M. Tarbell, "Closure Models for Turbulent Reacting Flows," *AIChE J.*, **35**, 2113 (1989).

Fox, R. O., "Computation of Turbulent Reactive Flows: First Principle Macro/Micro Mixing Models Using Probability Density Function Methods," *Chem. Eng. Sci.*, **47**, 2853 (1992).

Frisch, U., and S. A. Orszog, "Turbulence: Challenges for Theory and Experiment," *Physics Today*, **43**, 24 (1990).

Levenspiel, O., *Chemical Reaction Engineering*, 3rd Ed., Wiley, New York, p. 363 (1999).

Li, K. T., and H. L. Toor, "Turbulent Reactive Mixing with a Series-Parallel Reaction: Effect of Mixing on Yield," *AIChE J.*, **32**, 1312 (1986).

Madras, G., and B. J. McCoy, "Numerical and Similarity Solutions for Reversible Population Balance Equations with Size-Dependent Rates," *J. Colloid Interface Sci*., **246**, 356 (2002).

McCoy, B. J., and G. Madras, "Evolution to Similarity Solutions for Fragmentation and Aggregation," *J. Colloid Interface Sci.*, **201**, 200 (1998).

McCoy, B. J., and G. Madras, "Tracer Mixing Dynamics during Aggregation and Fragmentation," *AIChE J.*, **48**, 2167 (2002).

McCoy, B. J., and G. Madras, "Chemical Kinetics in Dispersed-Phase Reactors: Effects of Fragmentation and Coalescence," *Int. J. Chem. React. Eng.*, **1**, A10 (2003a).

McCoy, B. J., and G. Madras, "Analytical Solution for a Population Balance Equation with Aggregation and Fragmentation," *Chem. Eng. Sci.,* **58,** 3049 (2003b).

McCoy, B. J., and M. Wang, "Continuous-Mixture Fragmentation Kinetics: Particle Size Reduction and Molecular Cracking," *Chem. Eng. Sci.*, **49**, 3773 (1994).

Ottino, J. M., P. DeRoussel, S. Hansen, and D. V. Khakhar, "Mixing and Dispersion of Viscous Liquids and Powdered Solids," *Adv. Chem. Eng.*, **25**, 105 (1999).

Rietema, K., "Heterogeneous Reactions In The Liquid Phase," *Chem. Eng. Sci.*, **8**, 103 (1958).

Sundaresan, S., "Modeling the Hydrodynamics of Multiphase Flow Reactors: Current Status and Challenges," *AIChE J.*, **46**, 1102 (2000).

Szalai, E. S., J. Kukura, P. E. Arratia, and F. J. Muzzio, "Effect of Hydrodynamics on Reactive Mixing in Laminar Flows," *AIChE J.*, **49**, 168 (2003).

Manuscript received Mar. 12, 2003, and revision received Aug. 26, 2003.